JOURNAL OF MAGNETIC RESONANCE, Series B 104, 105–110 (1994)

# Simulation of Multiple Isotropic Spin-Trap EPR Spectra

DAVID R. DULING

*Laboratory of Molecular Biophysics, National Institute of Environmental Health Sciences, P.O. Box 12233, Research Triangle Park, North Carolina 27709*

Received March 26, 1993; revised August 20, 1993

**A computer program has been developed for fitting EPR data with multiple free radicals as formed in biochemical and chemical spin-trapping systems. Simulation of these spectra requires as many as 40 independent parameters, creating a chaotic analysis environment. Accurate simulation of these systems is essential for correct identification of the free radicals, which often show only slight differences in spin-Hamiltonian parameters. This method consists of rule-based perturbations with trial and error calculations and has proven successful in several applications. Details of the algorithm, example data, and a discussion of the difficulties of this analysis are presented in this report.** © 1994 Academic Press, Inc.

## INTRODUCTION

Spin trapping has proven very useful in the analysis of free radicals in biological samples (*1*); however, the simple molecular structure of a spin trap does not always lead to an easy analysis of the resultant EPR spectra. In biochemical systems, we frequently find that several independent free-radical species are trapped, leading to a superposition of very similar spectra. These species will often show only slight deviation of the critical hyperfine coupling constants (hcc), which are further obscured by the relatively wide detected linewidths. The ensuing analytical frustration has led us to develop a computer program for refining hypothetical simulation parameters to optimal values, allowing the researcher to test various possible free-radical formation pathways in a relatively unbiased manner. This program has been used in publications from this laboratory.

## CALCULATIONS

Individual simulations are calculated using the coefficients of the Fourier-transform (FT) spectrum (*2, 3*). The effects of the experimental modulation amplitude and time constant are included. In addition, we have included independent linewidth calculations for the $M = -1, 0, +1$ states of the nitrogen nucleus. The resulting equation has the form

$$\mathrm{FT}_f = M_f T_f \sum_{j=1}^{J} [R_f N_{f,j} \prod_{k=1}^{K} H_{f,j,k}], \qquad [1]$$

where the Fourier frequency $f$ ranges from 1 to $n/2$ ($n$ = number of data points), $J$ is the number of free-radical species, $K_j$ is the number of independent hyperfine coupling nuclei within each species, and $R_j$ is the relative amplitude of each species. The modulation amplitude and time constant are described by Eq. [2] and [3], respectively,

$$M_f = \sin(f\pi m/\Delta)/(f\pi) \qquad [2]$$

$$T_f = (t/s)[1 - i2\pi f(t/s)]/\{[2\pi(t/s)]^2 + 1\}, \qquad [3]$$

where $\Delta$ is the scan range in gauss, $m$ is the modulation amplitude, $t$ is the time constant, $s$ is the scan time, and $i = \sqrt{-1}$. The nitrogen hyperfine term has the form

$$N_{f,j} = \sum_{q=-1,0,1} [(L_{f,j,q} + G_{f,j,q})A_{f,j,q}], \qquad [4]$$

which is detailed by the equations

$$L_{f,j,q} = P_j f \exp(-2\pi f w_{j,q}/\Delta) \qquad [4a]$$

$$G_{f,j,q} = (1 - P_j) f \exp[-(2\pi f w_{j,q})^2/\Delta] \qquad [4b]$$

$$A_{f,j,q} = \exp[-i2\pi f(\Delta/2 - g_j - qx_j)], \qquad [4c]$$

where $P_j$ is the percentage Lorentzian component, $w_{j,q}$ is the linewidth at each quantum number, $g_j$ is the $g$ value measured as the offset from the center of the spectrum in gauss, and $x_j$ is the nitrogen splitting in gauss. The remaining hyperfine terms are represented by the following equations with $a_{j,k}$ as the hyperfine splitting in gauss:

$$H_{f,j,k} = \cos(\pi f a_{j,k}/\Delta), \quad \text{spin } 1/2 \qquad [5]$$

$$H_{f,j,k} = (2/3)[\cos(2\pi f a_{j,k}/\Delta) + 1/2], \quad \text{spin } 1 \qquad [5a]$$

$$H_{f,j,k} = (3/2)[\cos(2\pi f a_{j,k}/\Delta) + \cos(3\pi f a_{j,k}/\Delta)], \quad \text{spin } 3/2. \qquad [5c]$$

Equations [2] and [3] are constants for any single experiment and do not figure into the optimization complexity.



1064-1866/94 $6.00

The continuous-wave simulation is achieved by a simple inverse fast Fourier transform (FFT), followed by the error calculation:

$$CW = FFT^{-1}(FT) \quad [6]$$

$$Error = \sum_{f=1}^{n} [exp_f - CW_f]^2. \quad [7]$$

We can also minimize the error function in the FT domain:

$$EFT = FFT^{-1}[CW] \quad [8]$$

$$Error = \sum_{f=1}^{n/2} [EFT_f - FT_f]^2. \quad [9]$$

In the FT representation, Eq. [1], both the real and the imaginary components have significant intensities, while in the CW representation, Eq. [6], only the real component is significant. Equations [1]–[9] illustrate the challenging nature of optimizing these systems. To correctly simulate a

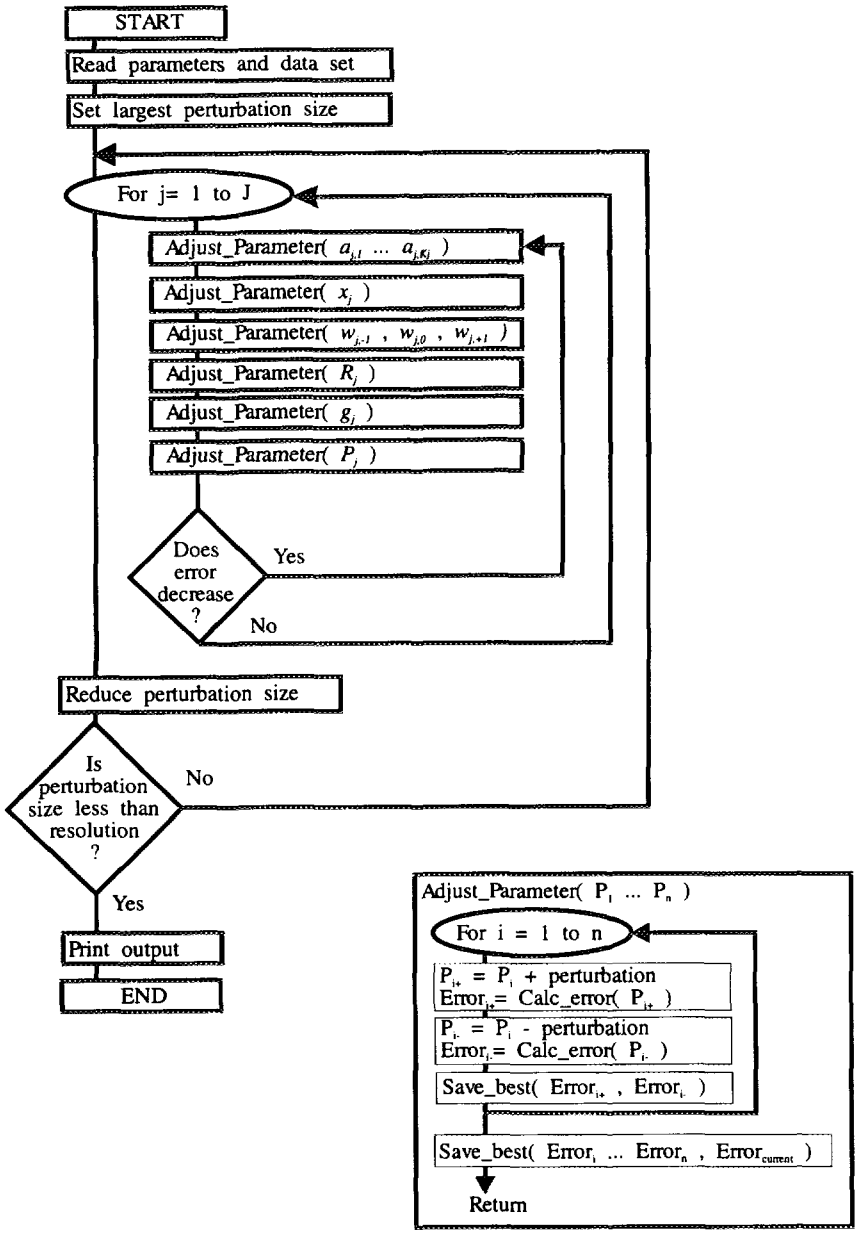


FIG. 1. Flow diagram of the LMB1 algorithm. The parameters are labeled as in the text under Methods. The number of free radical species is denoted by $J$. The program starts with a chosen large perturbation, adjusts each parameter individually, and calculates the new simulation and error value, repeating this process until the perturbation has been reduced to the spectral resolution (scan width/number of data points).

spectrum, we must minimize Eq. [7] or [9] for the following variables for each of the $J$ number of radical species: the nitrogen splitting constant $x_j$, the additional splitting constants, $a_{j,k}$, the relative intensity of each species, $R_j$, the $g$ value, $g_j$, the Lorentzian content of the lineshape, $P_j$, and the nitroxide linewidths, $w_{j,q}$. In biochemical systems, as many as five radical species have been observed, giving rise to 40 or more parameters to be optimized. This multidimensional error surface presents a challenging task to any minimization function; most of the local minima into which an algorithm can fall do not correspond to any viable chemical possibility. Many of the conventional minimization routines use derivative calculations to quickly descend the local minima structure; these derivatives are costly to compute and restrict the global search area. Any optimization of more than a few parameters requires careful selection of the initial quantities, regardless of the technique used.

## METHODS

Our method of optimizing the simulation, LMB1, evolved from an algorithm previously published, TUNE (*4*), for optimizing the simulation of a single free radical with a complex spectrum. LMB1 is specifically designed to optimize estimated spin-Hamiltonian parameters describing each spin adduct in a multicomponent spin-trap spectrum. It works equivalently in either the CW or the FT domains and attempts to treat Eq. [7] or [9] as an single quantity, rather than a combination of smaller functions for each radical species. LMB1 simply iterates through the spectral parameters, creating trial simulations and error calculations starting with large perturbations and ending with small perturbations. Its main points are: (i) the order of parameter testing is determined by the likely magnitude of its effect on the final spectrum fit; (ii) only a single parameter is varied at once; (iii) no parameter is changed more than once before all other parameters are tried; (iv) any parameter can be held constant; (v) the routine exits when all parameters have been tested at the best resolution; and (vi) any given combination of initial parameters and experimental spectrum will always

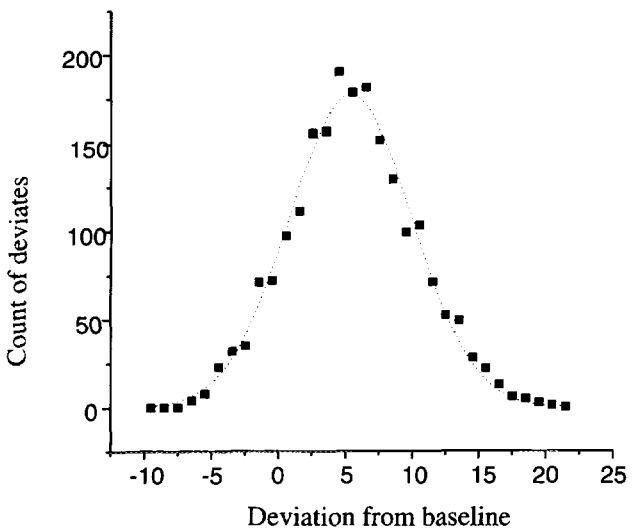


FIG. 2. Noise distribution from an EPR spectrometer with typical settings, taken at low magnetic field to avoid resonance signals. Spectrometer, Bruker ER200; sample, strong pitch; field center, 1000 G; scan range, 60 G; microwave power, 10 dB; receiver gain, $1E+6$; time constant, 1.25 ms; scan time, 10 min; modulation amplitude, 0.5 G. Gaussian fit is also shown with mean = 5.33 and standard deviation = 4.10.

TABLE 1
Results of Fitting DMPO/•OH and DMPO/•OOH Composite Spectrum

| | | Signal-to-noise ratio | | | | | |
|---|---|---|---|---|---|---|---|
| | | 5 | | 10 | | 50 | |
| | Actual value | LMB1 results | | | | | |
| | | $\mu$ | $\sigma$ | $\mu$ | $\sigma$ | $\mu$ | $\sigma$ |
| •OH | | | | | | | |
| aN | 15.30 | 15.28 | 0.006 | 15.28 | 0.020 | 15.29 | 0.029 |
| aH1 | 15.30 | 15.32 | 0.016 | 14.84 | 1.010 | 15.34 | 0.137 |
| aH2 | 0.61 | 0.61 | 0.003 | 0.66 | 0.007 | 0.61 | 0.008 |
| aH3 | 0.25 | 0.14 | 0.091 | 0.61 | 0.866 | 0.24 | 0.037 |
| •OOH | | | | | | | |
| aN | 14.30 | 14.30 | 0.003 | 14.29 | 0.036 | 14.30 | 0.005 |
| aH1 | 11.70 | 11.70 | 0.005 | 11.70 | 0.007 | 11.70 | 0.007 |
| aH2 | 1.25 | 1.24 | 0.005 | 1.24 | 0.006 | 1.25 | 0.010 |
| $R$ | | 0.957 | | 0.983 | | 0.999 | |
| $n$ | | 940 | | 949 | | 725 | |
| | | Simplex results | | | | | |
| | | $\mu$ | $\sigma$ | $\mu$ | $\sigma$ | $\mu$ | $\sigma$ |
| •OH | | | | | | | |
| aN | 15.29 | 15.29 | 0.035 | 15.28 | 0.045 | 15.29 | 0.007 |
| aH1 | 15.30 | 15.31 | 0.108 | 15.35 | 0.104 | 15.30 | 0.016 |
| aH2 | 0.63 | 0.62 | 0.023 | 0.64 | 0.015 | 0.61 | 0.008 |
| aH3 | 0.25 | 0.25 | 0.018 | 0.25 | 0.008 | 0.26 | 0.020 |
| •OOH | | | | | | | |
| aN | 14.30 | 14.29 | 0.015 | 14.30 | 0.005 | 14.30 | 0.006 |
| aH1 | 11.70 | 11.71 | 0.026 | 11.69 | 0.016 | 11.69 | 0.008 |
| aH2 | 1.25 | 1.24 | 0.016 | 1.24 | 0.022 | 1.26 | 0.002 |
| $R$ | | 0.956 | | 0.987 | | 0.994 | |
| $n$ | | 920 | | 1129 | | 2003 | |

*Note.* Results of fitting the DMPO/•OH and DMPO/•OOH spectrum with the LMB1 and Simplex algorithms for the hyperfine coupling constants (hcc) are shown. Three reference spectra were created with $S/N$ values of 5, 10, and 50 using a Gaussian noise-generating function. Four starting parameter sets were generated with initial parameters created as a Gaussian distribution with $\mu$ = true_value and $\sigma$ = 0.05 (true_value). The hcc-fitted mean ($\mu$) and standard deviation ($\sigma$) are shown at each $S/N$ ratio, although the linewidth, lineshape, $g$ value, and relative concentration parameters were also fitted. Also shown is the average rank correlation constant ($R$) of the final simulations and the average number of calculations ($n$) needed at each $S/N$ ratio.

produce the same result. The complete algorithm is presented in Fig. 1. LMB1 is not based on a standard numerical "recipe" with interpolations and derivatives and, as such, could not be applied as is to other problems, although analogous procedures could be devised.

For comparison, we show the well-known Simplex (*5*) method of functional minimization. Simplex is a nonderivative-based algorithm that performs a multidimensional interpolation of all parameters at each iteration, in contrast to LMB1. If $P$ is the number of parameters to be optimized, then Simplex requires $P + 1$ initial simulations with differing parameter sets. After choosing initial parameters, we generate the remaining $P$ starting sets as Gaussian (normal) deviates,

$$\text{par}_{p,s} = N(\mu = \text{par}_{p,1}, \sigma = 0.05\ \text{par}_{p,1}), \qquad [10]$$

where $p$ ($1 \leq p \leq P$) is the parameter number, and $s$ ($2 \leq s \leq P + 1$) is the Simplex perturbation number. The actual deviations are generated by a published (*6*) Gaussian random number generator. Notice that, since this Simplex is a function of a random numbers, a given combination of initial parameters and data set will not produce identical output. Simplex exits when a predefined fractional tolerance (ftol) has been achieved. Typically, a Simplex is reinitialized and restarted after ftol has been met a few times before a final tolerance is accepted. The ftol is defined in Eq. [11], where max and min are both retrieved from an array of the P + 1 best errors.

$$\text{ftol} = 2|\text{max} - \text{min}|/(|\text{max}| + |\text{min}|). \qquad [11]$$

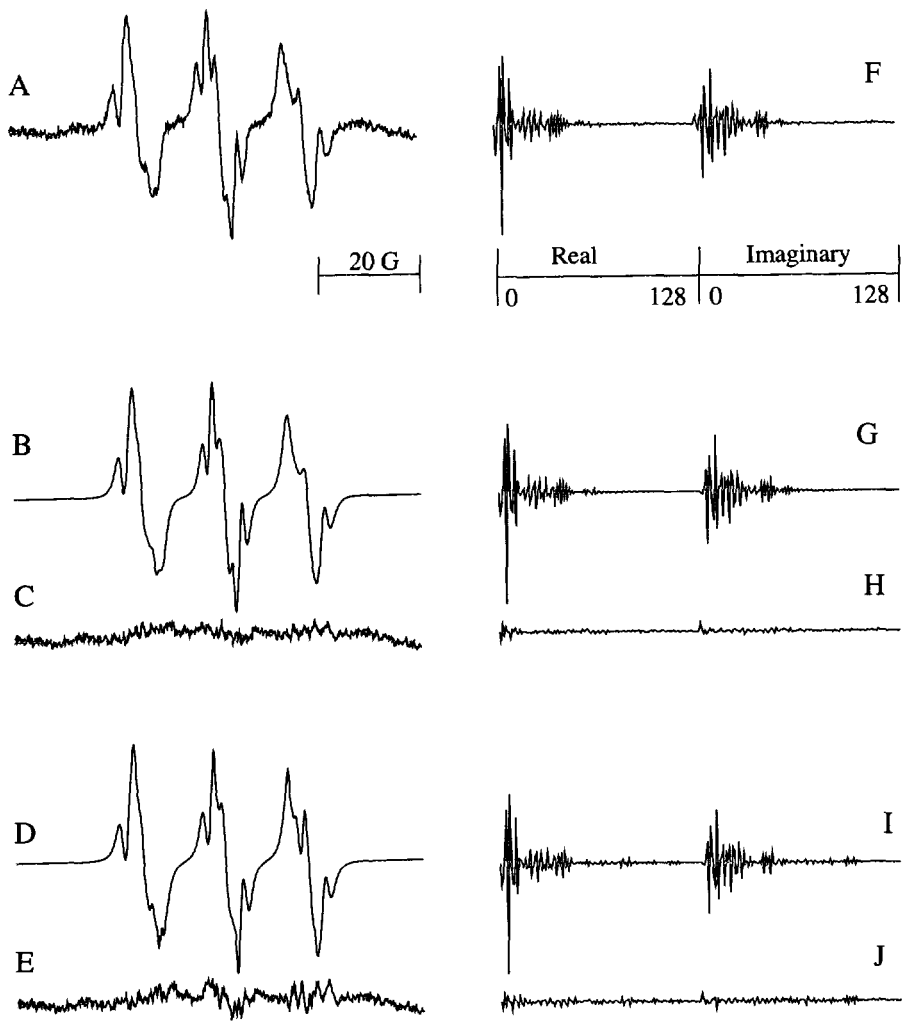


FIG. 3. Continuous-wave (CW) and Fourier-transform (FT) fit results for the five-species, 40-parameter model with the final correlation constant ($R$) and number of calculations ($n$). Both the CW and the FT results are shown. The FT is defined as FT = FFT(CW). (A) CW experimental spectrum; scan range, 80.0 G; data points, 2048; resolution, 0.04 G/point. (B) CW-LMB1 final simulation; $R$ = 0.994; $n$ = 5457. (C) CW-LMB1 residual spectrum. (D) CW-Simplex final simulation; $R$ = 0.987; $n$ = 8270. (E) CW-Simplex residual. (F) FT experimental spectrum, shown as the first 128 data points of both the real and imaginary domains although the resolution remains 0.04 G/point. (G) FT-LMB1 final simulation; $R$ = 0.993; $n$ = 3601. (H) FT-LMB1 residuals. (I) FT-Simplex final simulation; $R$ = 0.986, $n$ = 8597. (J) FT-Simplex residuals.

## RESULTS

A measured CW EPR spectrum should be the sum of the actual signal and normally distributed noise with mean and variance dependent on the spectrometer settings.

$$\exp = \mathrm{CW} + \epsilon, \quad \epsilon \sim N(\mu_0, \sigma_0). \qquad [12]$$

In fact, baseline data acquired from our instruments demonstrates this relationship, as shown in Fig. 2. Given the normal distribution of acquired data, the spin-Hamiltonian parameter estimates resulting from a numerical fit should have their own normal distributions; using repetitive trials, one can produce estimates of the parametric means and standard deviations. Without repetitive trials, this is a difficult estimation.

The first example is of the (5,5-dimethyl-1-pyrroline *N*-oxide) DMPO/$^{\bullet}$OH and DMPO/$^{\bullet}$OOH composite spectrum with parameters published by Bolton (*7*). A noise pattern with a normal distribution ($\mu = 0.0$, $\sigma = 1.0$) was created and a simulated signal added at intensities 5, 10, and 50, creating those signal-to-noise ($S/N$) ratios. The spectrum width consists of 60 G over 2048 data points, yielding a resolution of 0.03 G/point. This test used a constant linewidth. Four sets of initial parameters were then created with deviations distributed normally [$\mu$ = true_value, $\sigma = 0.05$ (true_value)] to test the program at each $S/N$ ratio with both the LMB1 and the Simplex routines. Table 1 summarizes the 24 sets of results: the mean and standard deviations at each $S/N$ are generally good and positively identify the radical spectra. The average correlation constant at each $S/N$ is quite good. While the accuracy improves as the $S/N$ increases for both methods, the programs are usually able to extract the correct parameters even with bad inputs and poor signals.

The second example shows data recently published (*8*) involving a very complex five-species, 40-parameter spectrum of the (*N*-*t*-butyl-$\alpha$-phenylnitrone) PBN spin trap that demonstrates significant nitrogen quantum-dependent linewidths, poor resolution of hyperfine features, and a deviant baseline. The spectral width is 80 G over 2048 data points, yielding a resolution of 0.04 G/point. The spectrum was fitted using both the LMB1 and Simplex methods, producing apparently good results, as shown in Fig. 3; however, the LMB1 algorithm produced somewhat better correlation values in fewer iterations. Also, the spectrum was modeled as both CW and FT data and while the number of iterations is comparable between the CW and FT tests, the more efficient calculations of the FT jobs produces run times an order of magnitude shorter (using Eqs. [1]–[9]), a value that is independent of the computer used. The final parameters (Table 2) show deviations between the CW and FT domains and between the LMB1 and Simplex methods with the radical assignments based on the hyperfine coupling constant results of the LMB1 algorithm applied to CW data. Hyperfine couplings from the alternate fits show differences as large as ~1 G, which are significant enough to alter interpretation. To investigate this dilemma, we searched the Spin Trap Data Base (*9*) for the highly characteristic PBN/$^{\bullet}CO_2^-$ radical adduct (clearly evident in other spectra but not in Fig. 3A) with the range of $a^N$ and $a^H$ set to the fit result ±0.3 G. The interval was chosen to be large enough to include normal parameter deviation while excluding most alternative hypotheses and is significantly larger than the resolution of the experiment. The CW-LMB1 result yielded 31 references; CW-Simplex, 0; FT-LMB1, 1; and FT-Simplex, 0. These results imply that the CW-LMB1 fit is most believable. Linewidth and lineshape results are not appropriate for radical identification; however, badly erroneous values may point to useless simulations. The paradox of apparently excellent fits producing competing assignments illustrates the com-

TABLE 2
**Fitting Results for the Five-Species/40-Parameter PBN Spectrum**

| | CW-LMB1 | CW-Simplex | FT-LMB1 | FT-Simplex |
|---|---|---|---|---|
| $^{\bullet}{}^{13}CH_3$ | | | | |
| Concentration | 53.000 | 40.323 | 49.000 | 41.090 |
| aN | 16.407 | 16.128 | 16.378 | 16.060 |
| aH | 3.360 | 3.474 | 3.473 | 3.456 |
| aH | 4.000 | 4.266 | 3.955 | 4.048 |
| $^{\bullet}O\ {}^{13}CH_3$ | | | | |
| Concentration | 32.000 | 36.925 | 36.000 | 25.536 |
| aN | 15.635 | 15.745 | 16.085 | 15.599 |
| aH | 3.060 | 3.292 | 2.827 | 3.004 |
| $^{\bullet}Y$ | | | | |
| Concentration | 22.000 | 11.196 | 36.000 | 12.115 |
| aN | 15.325 | 15.468 | 14.980 | 15.447 |
| $^{\bullet}C(O)R$ | | | | |
| Concentration | 2.500 | 2.511 | 3.000 | 2.103 |
| aN | 15.766 | 16.641 | 15.444 | 15.550 |
| aH | 3.360 | 2.947 | 3.995 | 4.371 |
| $^{\bullet}CO_2^-$ | | | | |
| Concentration | 1.500 | 0.952 | 1.000 | 1.342 |
| aN | 15.719 | 14.621 | 16.002 | 15.571 |
| aH | 4.360 | 4.230 | 4.096 | 5.746 |

*Note.* Resulting parameter estimates for the example PBN spectrum using both the LMB1 and the Simplex algorithms in both CW and FT domains are shown. The model included five free radical species, each with a relative intensity, isotropic $g$ value, three linewidths for the $-1$, 0, $+1$ quantum nitroxide states, and hcc for a total of 40 independent parameters for fitting. Only the relative concentration and critical hyperfine coupling constants are shown although the linewidth, lineshape, $g$ value, and relative concentration parameters were also fitted. A wide deviation in the hcc estimates is demonstrated between the LMB1 and Simplex as well as between the CW and FT domains. These values were corroborated with the Spin Trap Data Base (see text); the CW-LMB1 results were used in the given assignment of parameters.

plexity of the task and the necessity of exhaustive experimentation with extensive analysis. That said, we note that the chosen simulation did in fact produce a higher correlation constant and better residual distribution.

## DISCUSSION

The LMB1 algorithm has proved itself to be very useful in our work, eliminating many tedious hours of simulation refinement. These programs provide a research tool for testing one hypothesis versus another, using error estimates and published data such as the Spin Trap Data Base. With a very complex spectrum of many species, these programs can eliminate a poorly chosen hypothesis; however, results are very dependent on initial parameters. Therefore, the researcher must be able to produce credible models and use optimization programs as hypothesis testers. In particular, refinement along the lineshape–linewidth grid is difficult; fortunately, these parameters are not usually critical to the identification of the radical. The researcher retains responsibility for discriminating between competing models on the basis of his or her own knowledge of the field. No data-analysis technique is a substitute for a good understanding of the chemistry underlying the experiment. Finally, although results from the Simplex algorithm were reported, this report is not intended as a comparison, but rather to establish the LMB1 algorithm as a legitimate and convenient means of analyzing EPR spectra.

## AVAILABILITY OF COMPUTER PROGRAMS

Versions of these programs compiled for the IBM PC-compatible DOS computer are available electronically and by surface mail; the author may be contacted for details.

## ACKNOWLEDGMENTS

Dr. Philip M. Hanna provided experimental spectra and useful discussions on their analysis and interpretation. Doren Yen and Kevin Kirkeby both coded portions of the analysis programs used in this report.

## REFERENCES

1. C. Mottley and R. P. Mason, *Biol. Magn. Reson.* **9,** 489–546 (1989).
2. J. C. Evans, P. H. Morgan, and R. H. Renaud, *Anal. Chim. Acta.* **103,** 175–187 (1978).
3. W. R. Dunham and J. A. Fee, *J. Magn. Reson.* **40,** 351–359 (1980).
4. A. Motten and J. Schreiber, *J. Magn. Reson.* **67,** 42–52 (1986).
5. W. H. Press, B. P. Flannery, S. A. Teukolsky, and W. T. Vetterling, pp. 289–294, Cambridge Univ. Press, London/New York, 1986.
6. W. H. Press, B. P. Flannery, S. A. Teukolsky, and W. T. Vetterling, pp. 200–203, Cambridge Univ. Press, London/New York, 1986.
7. J. R. Harbour, V. Chow, and J. R. Bolton, *Can. J. Chem.* **52,** 3549–3553 (1974).
8. M. J. Burkitt, M. B. Kadiiska, P. M. Hanna, S. J. Jordan, and R. P. Mason, *Mol. Pharmacol.* **43,** 257–263.
9. A. S. W. Li, K. B. Cummings, H. P. Roethling, G. B. Buettner, and C. F. Chignell, *J. Magn. Reson.* **79,** 140–142 (1988).